Original Article

Development of 3D-QSAR Models to Predict Inhibition Activity of Selective Histone Deacetylase 1-3 Inhibitors

Narges Cheshmazar, Amirhossein Nasri, Siavoush Dastmalchi

DOI: 10.34172/PS.025.42810

To appear in: Pharmaceutical Science (https://ps.tbzmed.ac.ir/)

Received date: 9 Jun 2025

Revised date: 27 Aug 2025

Accepted date: 17 Sep 2025

Please cite this article as: Cheshmazar N, Nasri A, Dastmalchi S. Development of 3D-QSAR models to predict inhibition activity of selective histone deacetylase 1-3 inhibitors. Pharm Sci. 2026. Doi: 10.34172/PS.025.42810

Development of 3D-QSAR models to predict inhibition activity of selective histone deacetylase 1-3 inhibitors

Narges Cheshmazar[1†https://orcid.org/0000-0002-9998-8121], Amirhossein Nasri[2†https://orcid.org/0009-0006-9537-4890], Siavoush Dastmalchi[1,2,3https://orcid.org/0000-0001-9427-0770]

[1]Biotechnology Research Center, Tabriz University of Medical Sciences, Tabriz, 5165665813, Iran;

[2]Department of Medicinal Chemistry, School of Pharmacy, Tabriz University of Medical Sciences, Tabriz, 5166414766, Iran;

[3]Faculty of Pharmacy, Near East University, PO Box 99138, Nicosia, North Cyprus, Mersin, 10, Turkey.

*Author for correspondence: dastmalchi.s@tbzmed.ac.ir

†These authors contributed equally as first authors: Narges Cheshmazar and Amirhossein Nasri

Abstract

Background: Histone deacetylase inhibitors (HDACIs) have attracted researchers' attention as anti-cancer agents. Designing novel HDAC inhibitors is important in drug discovery field of HDAC due to their high potency, less off-target effects, and good pharmacokinetic and pharmacodynamic profiles. 3D quantitative structure-activity relationship (3D-QSAR) is a computational method used to design novel compounds considering 3D structure of molecules.

Methods: In the current study, we have performed two successive QSAR analyses including a classification based for recognizing selective HDAC1-3 inhibitors from non-selective inhibitors and a 3D-QSAR to predict the potency of inhibitors. To this, initially a classification based QSAR was developed to filter selective HDAC1-3 inhibitors from other isoform-selective or pan inhibitors. Also, a receiver operating characteristics (ROC) analysis was performed for evaluation the goodness of classification model performance. Then, three different 3D-QSAR models were developed specifically for the filtered selective HDAC1-3 inhibitors to assess their selectivity and potency.

Results: The generated models revealed that some common structural moieties have positive or negative effect towards the potency of the studied compounds against all three HDAC 1-3 isoforms. The results indicated that out of the identified important variables, a variable named DRY-TIP showing the optimum distance between ZBG and cap group. Furthermore, presence of two HBD groups in ZBD to form pseudoring with a zinc ion present in the active site of the enzyme are essential for exerting inhibitory activity. Using partial least square analysis, a 3D-QSAR model with 5 latent variables was generated with q^2 values of internal and external validation equal to 0.62, 0.84, 0.83 and 0.72, 0.90, 0.82 for HDAC1,2,3, respectively.

Conclusion: The result of the current study can be used to recognize selective HDAC1-3 inhibitors and predict their potencies with the aim of selective HDAC1-3 inhibitor design.

Keyword: Histone deacetylase, selective HDAC1-3 inhibitor, GRIND, 3D-QSAR, Docking, Classification.

1. Introduction

Acetylation of lysine residue in histone proteins results in the removal of the positive charge of the ε-amine group weakening histone-DNA binding and consequently leading to the relaxed form of the chromatin. In contrast deacetylation leads to rigidity of the chromatins. The regulatory role of acetylation and deacetylation balance is important in diverse biological processes specifically in gene transcription.[1,2] Histone deacetylases (HDACs) leads to suppression of gene expression through deacetylation of lysine residue on histone tails.[3,4] Until now, 18 human HDACs have been recognized in which their classification was based on their sequence, structure, location, and function.[5] There are two main categories including Zn^{2+}-dependent isoenzymes comprising class I (HDAC1-3 and 8), class II (HDAC4-7, 9, and 10) and class IV (HDAC11), and NAD^{+}-dependent isoenzymes which constitute class III (SIRT1-7) of HDAC isoforms.[6-8] All HDAC isoenzymes have three main sections in terms of zinc binding domain (ZBD), hydrophobic channel, and outer rim which are located in the bottom, wall, and surface area of active site.[9] Different investigations indicated that HDACs are overexpressed in variety of diseases encompassing cancer, Alzheimer, neurological diseases, inflammatory diseases, and metabolic disorders.[6,10,11] HDAC1 is overexpressed in prostate, gastric, colon, and breast carcinomas, while the overexpression of HDAC2 is majorly observed in colorectal, cervical and gastric cancers, and HDAC3 is mainly expressed in colon tumor.[12] Based on results of clinical trials, HDACs inhibitors (HDACIs) displayed hopeful therapeutic effects in therapy of cancer and Alzheimer specifically.[13-16] Currently, there are three major class of HDACIs including pan or nonselective HDACIs (such as vorinostat (SAHA), panobinostat (LBH-589), belinostat (PXD-101), valproic acid (VPA)),[17,18] selective HDACIs (such as class I selective HDACIs (romidepsin and entinostat)) and multitarget HDACIs (including CUDC-

101 and CUDC-907).[19] Studies showed that selective HDACIs have more potency, less off-target effects, and better pharmacodynamics and pharmacokinetic profiles compared to pan inhibitors.[20] Hence, development of isoform-selective HDACIs has attracted research interests in this field.[21] From structural point of view, the molecular structures of HDAC inhibitors can be divided into three main sections including cap, linker, and ZBG. To date, for the majority of HDAC1-3 selective inhbitors, the ZBG is either benzamide[22] or hydrazide,[23] while the linker group is cyclic. Quantitative structure–activity relationship (QSAR) technique is a drug design and discovery method which is extensively conducted to correlate structure features (defined as descriptors) and biological activities for a set of molecules.[24] QSAR has different applications but mostly is being used for designing novel and potent compounds as well as predicting the biological activities.[25] QSAR analyses can be categorized based on different criteria. For example, based on the dimensionality of the descriptors, the type of QSAR models can range from 0D- to 7D-QSAR.[26,27] In 3D-QSAR methods, the main focus is on spatial parameters, three-dimensional structures, and stereochemical properties.[28,29] 3D-descriptors are employed in alignment-dependent (aligning studied compounds with each other) and alignment independent 3D-QSAR approaches, however the latter approach is more useful, which may be due to the complexity of the molecular alignment process in the case of structural heterogeneity.[30] In one form of alignment-independent methods called GRid-Independent Descriptors (GRIND),[30,31] molecular interaction fields (MIF) are calculated to describe the interaction energy between ligands and different types of probes.[32] As a result, the high numbers of calculated descriptors were analyzed based on their impact on the biological activity to determine favorable and unfavorable interactions.[33] Due to the problems associated with existing selective HDAC1-3 in market such as

entinostat, there are need to design and develop novel selective HDAC1-3 inhibitors with modified potency and improved pharmacodynamic properties. Here, we developed a 3D-QSAR model on selective HDAC1-3 inhibitors to predict their biological activity and design novel inhibitors. To this aim, first, a series of HDACIs were collected from the literature, then, a classification based QSAR was performed in order to classify selective HDAC1-3 inhibitors. Subsequently, a 3D-QSAR model was developed and validated followed by performing a docking investigation to study receptor-ligand interaction.

2. Methods and Materials

2.1. Dataset preparation

A set of 121 HDAC 1-3, 6, and 8 inhibitors based on hydroxamic acid, benzamide, and hydrazide scaffolds (Table S1) were collected from the literature for 3D-QSAR studies.[23,34-42] All reported inhibitory activities were the IC_{50} values for inhibiting recombinant human HDAC enzyme. The biological activity values were converted to pIC_{50} (-log IC_{50}) and used as the dependent variable in the 3D-QSAR study. Then, the 3D structures of all selected compounds were generated using the Built Optimum option in HyperChem software (version 8.0.10). Subsequently, the generated structures were energy minimized using the MM+ force field based on Polack-Ribiere algorithm.[43] Then, the structures were fully optimized based on the semiempirical quantum mechanics AM1 method, available in HyperChem.[44] The output structures were converted to SYBYL Cartesian coordinate files (mol2 file format) using OpenBabel software (version 2.3.2).[45]

2.2. Classification of the dataset

To categorize all under study compounds as selective and nonselective HDAC1-3 inhibitors, first a classification-based QSAR analysis was performed. To aim this, DTC Lab Software Tools (https://teqip.jdvu.ac.in/QSAR_Tools/) proposed by Roy et al[46] was used. Initially, descriptors for all 121 compounds were calculated in Dragon software (version 5.5). Then, an input file including compounds number, class (1 for selective compounds and 0 for other compounds), calculated descriptors, and correspond pIC_{50} (see Table S1) for each compound was prepared to develop classification model using in DTC-QSAR_v1.0.7 tool.

2.3. Docking-based alignment

To determine active conformation of the 43 HDAC1-3 selective inhibitors from previous step, they were docked onto the active site of HDAC2. Among HDAC1, 2, and 3, just HDAC2 was cocrystallized with an HDAC inhibitor (SAHA) and since they have high similarity percent, HDAC2 was selected for docking study.[47] First, structure of HDAC2 enzyme (PDB ID: 4LXZ) was downloaded from the Protein Data Bank (http://www.RCSB.org). Then, the enzyme structure pretreated by retaining a single chain of the enzyme, energy minimizing its structure, and removing residue clashes using DeepView (Version 4.1.0) software.[48] The ligand binding pocket was defined by selecting residues within the 6 Å of the co-crystalized vorinostat (SAHA). The selected residues were Gly32, His33, Pro34, Met35, Glu103, Asp104, His145, His146, Gly154, Phe155, Cys156, Asp181, Ile182, His183, His184, Phe210, Gln265, Asp269, Arg275, Leu276, Gly305, Gly306, Gly307, and Tyr308. Then, flexible docking of selected compounds into the binding site of the enzyme was performed using GOLD (version5.0; CCDC Inc., Cambridge, UK) running on a LINUX operating system.[49,50] The coordination of the geometric center includes X: 39.9370, Y: 5.2070, and Z: -36.1460. By applying the default settings in GOLD, the best scoring

function (ASP) was selected based on the results of reproducing the experimentally known pose of SAHA in the binding site of HDAC2. Furthermore, for ensuring similar proper orientation of all compounds, two distance constraints were applied, i.e., setting the distances between Zn^{2+} ion to oxygen atom of carbonyl group and nitrogen atom of NH group in ZBG to 1.5 - 3.5 Å. In order to select optimal conformation for 3D-QSAR modelling, we examined the binding modes and orientations of the dataset ligands docked into the HDAC2 active pockets. Only those conformations with top ranked ASP values and with proper coordination of ZBG relative to Zn^{2+} ion (in bidentate fashion) in the catalytic domain were selected. Final selection of optimal bioactive conformations for QSAR modeling was based on the optimal orientation of the ligands in the active site and also presence of favorable interactions between ligands and amino acid residues at the outer rim of the active pocket identified essential according to previous observations.[51]

2.4. Calculation of GRIND and 3D-QSAR models building

The Pentacle software (Version 1.0.6, Molecular Discovery, Hertfordshire, UK) was used for calculating alignment-independent three-dimensional GRID-based molecular descriptors (GRIND, which stands for Grid-Independent Descriptors) and developing the 3D-QSAR models. First, the obtained active conformations of selected compounds were introduced to Pentacle program for producing GRIND-based descriptors. The molecular interaction fields (MIFs) were generated using GRIND based fields[32] by calculating the interaction energies at grid points called nodes between the compounds and different probes followed by removing the nodes with the energies below the default cut-off values. The probes used for generating MIFs such as DRY, HBA, HBD, and TIP for calculating hydrophobic, H-bond acceptor, H-bond donor, and steric

interactions, respectively. Then the most favorable GRIND descriptors were selected using AMANDA algorithm.[52] The obtained variables were then used for generating correlograms in which the product of node-node energies is represented against the distances between the nodes. Three 3D-QSAR models were developed for selected HDAC1-3 inhibitors based on HDAC1, 2, and 3 inhibition activities (pIC_{50}). To develop 3D-QSAR models, initially the 43 selective HDAC1-3 inhibitors were divided randomly to two train (N: 35) and test (N: 8) sets for HDAC 1, 2, and 3, using SPSS (v.27.0.1) software. The train set was used for construction of 3D-QSAR models to predict activities of test set. The selected variables were used to build 3D-QSAR models using partial least square (PLS) methodology.

2.5. Statistical analysis of constructed models

The generated models were checked from the quality point of view by internal cross validation methods. Fractional factorial design (FFD) method was employed to extract the most relevant variables to the compounds activities. FFD selection was repeated several times on the models until no improvement in the statistical parameters (R^2, Q^2 and SDEP values) was observed. Validity of the final models was evaluated using both internal (using leave-one-out (LOO) method) and external cross-validation methods. The predictively of the models was also assessed by calculating the standard deviation of the error of prediction (SDEP). All statistical analysis was performed by pentacle software.

3. Results and Discussion

The main object of this study is to develop 3D-QSAR models in order to predict the inhibition potency of selective HDAC1-3 inhibitors. To aim this, first 121 HDACIs compounds and their pIC_{50} values were collected from the literature, and introduced to Roy's QSAR tools to select selective

HDAC 1-3 inhibitors. Based on result of classification, a set of 43 selective HDAC1-3 inhibitors with benzamide and hydrazide scaffold (Table 2) were selected. The obtained results would be useful for identification of new selective inhibitors of HDAC1-3 isoenzymes in drug design studies. In the current study, first an alignment docking study was performed on the classified selective HDAC1-3 inhibitors to get the active conformation of the compounds (Figure 1). Then, the obtained conformations were introduced to pentacle software along with their pIC_{50} values to calculate MIFs around the active conformation of dataset ligands. Then, the energy of node-node in a specific distance of ligands was used for generating GRIND variables. Subsequently, the 3D-QSAR models were developed using GRIND descriptors as independent variables and the experimental HDAC2 inhibition (pIC_{50}) as dependent variables using PLS regression. The developed models were evaluated by internal and external validation approaches.

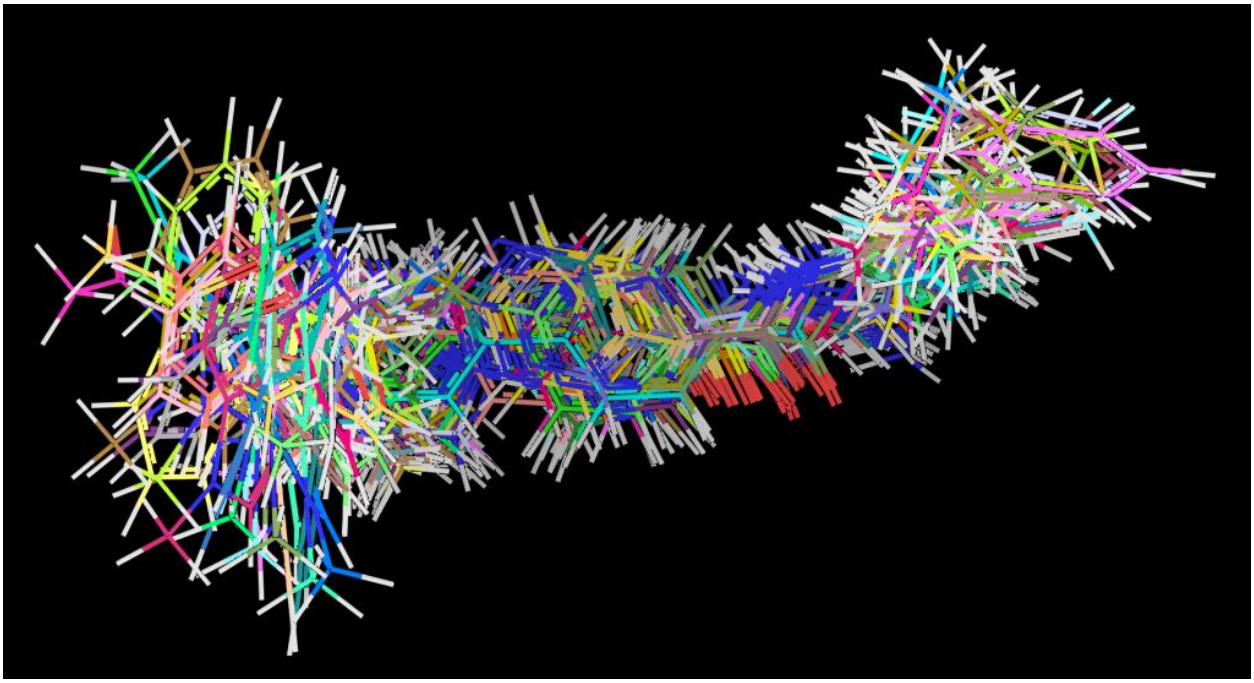

Figure 1. Docking based alignment of 43 selective HDAC 1-3 inhibitors to achieve the active conformation of the compounds.

3.1. Classification of compounds

The DTC-lab tool was used to classify compounds as selective and nonselective HDAC1-3 inhibitors. The software divided the dataset compounds into train (85 compounds) and test (36 compounds) sets. Based on the defined classification for the train set compounds, this tool predicted class for all compounds containing test and train sets according to Genetic Algorithm-Linear Discriminant Analysis (GA-LDA) model. The results are shown in Table S1 as well as validation metrics for classification based QSAR are shown in Table1. A confusion matrix which indicates the prediction power level of a classification model has four categories including correct predictions for both classes (true positives and true negatives) and incorrect predictions (false positives and false negatives). According to QSAR/QSPR Modeling Fundamental Concepts by Roy et al,[53] for a good classification model, all performance criteria should be near to 100 percent except for F-measure which should be near to unity. The MCC (Matthews's correlation coefficient) values were classified to three groups including +1 (represents a perfect prediction), 0 (demonstrates almost a random prediction) and −1 (indicates total disagreement between prediction and observation). Based on defined concepts and measures in the note of Table 1, all validation parameter of the constructed classification model are in acceptable range. Furthermore, the predictive power of the developed classification-based QSAR was assessed via receiver operating characteristics (ROC) analysis (Figure2). The receiver operating characteristics (ROC) curve was employed to measure the overall performance of a classification model through the calculation of the area under the curve (AUC) and plotting the true positive rate (sensitivity) against the false positive rate (specificity). The closer the ROC curve is to the top-left corner of the graph, the better the model's ability to distinguish between positive and negative classes. In this context, the AUC value for train and test sets were 0.86697 and 0.884615, respectively. These

results showed that this tool could predict the class of studied compounds correctly with high percentage of success which could be used to predict the selectivity of query compounds. Total of 43 compounds as selective HDAC1-3 inhibitors were entered to the next step (Table S1 and Table2).

Table 1. Validation metrics for classification based QSAR.

	Accuracy	Precision	Sensitivity	Specificity	F-Measure	MCC
Train	92.94%	96.15%	83.33%	98.18%	0.89	0.84
Test	91.66%	85.71%	92.30%	91.30%	0.89	0.82

Accuracy is defined as the fraction of correct prediction obtained for both the positive and negative observations with respect to the a priori defined class. **Sensitivity** or true positive rate, measures the ability of a model to correctly identify true positives. **Specificity** measures the proportion of negatives that are correctly identified by a model. **Precision** is defined as the fraction of correct prediction for the positive samples with respect to the total number of samples predicted as positives. **F-measure** is defined as 2 / (1/Precision + 1/Sensitivity). The Matthews correlation coefficient (**MCC**) defined as a balanced measure which can be used even if the classes are of very different sizes.

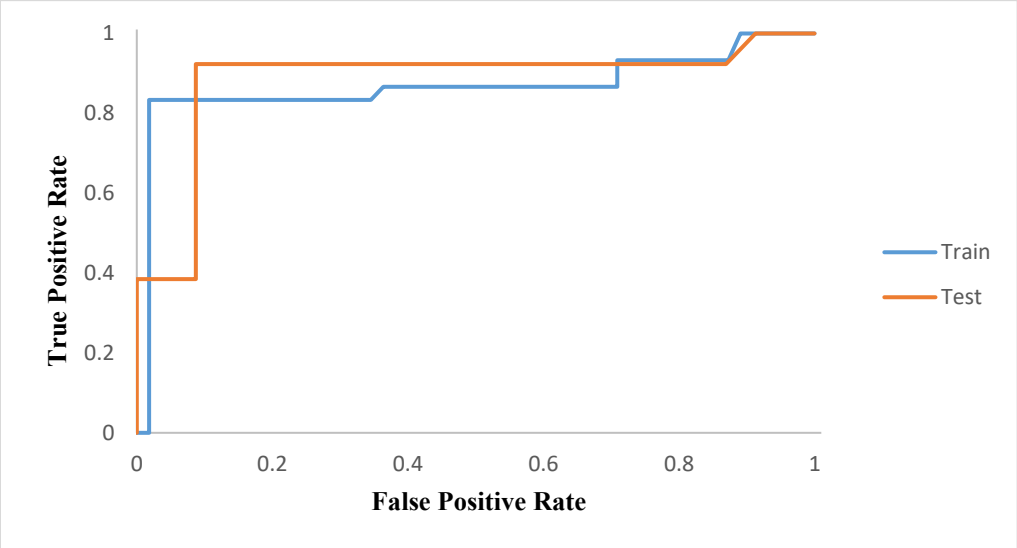

Figure 2. The results of Receiver Operating Characteristic (ROC) analysis and the corresponding Area Under the Curve (AUC) illustrating the performance of the developed classification based QSAR model.

Table 2. Structures of selective HDAC1-3 inhibitors associated with their experimental and predicted values.

		Activity (pIC_{50})					
		Experimental			Predicted		
Number	**Structure**	HDAC1	HDAC2	HDAC3	HDAC1	HDAC2	HDAC3
78	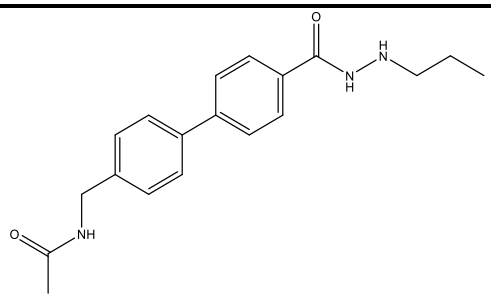	5.80	6.200	7.040	6.38	6.239	6.215

79	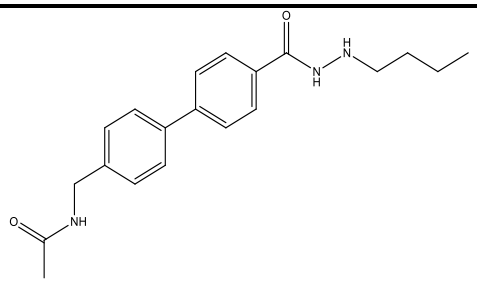	6.208	5.959	6.456	6.138	5.944	6.53
80	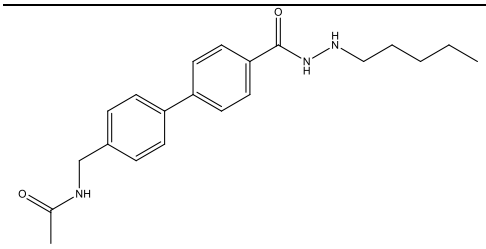	6.180	5.699	5.824	6.258	5.778	5.975
81	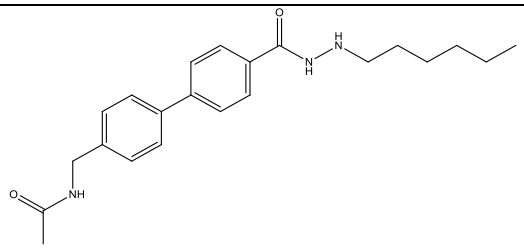	5.745	4.921	4.301	5.715	5.12	5.478
82	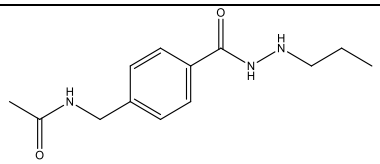	5.796	5.260	5.799	5.977	5.001	5.751
83	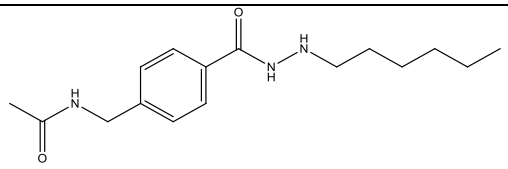	5.319	4.921	4.301	5.909	4.888	4.192
84	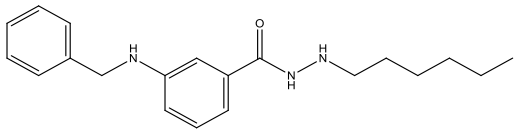	4.301	4.301	4.301	5.272	4.304	4.429

85	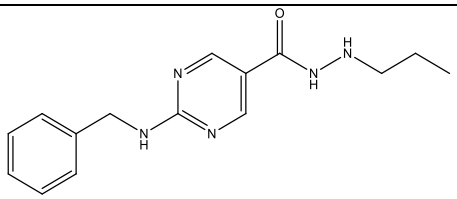	6.602	6.155	7.366	5.395	5.845	7.153
86	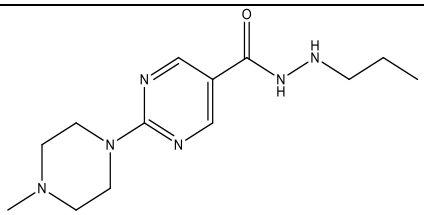	6.229	5.620	6.921	6.243	5.636	6.93
87	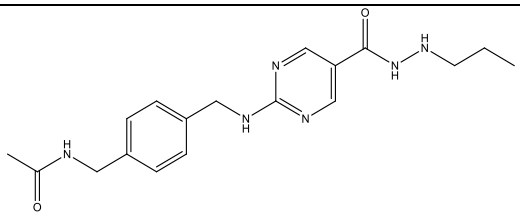	6.538	6.036	6.959	6.409	5.988	6.799
88	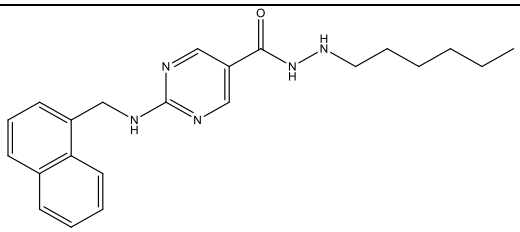	5.081	4.301	4.301	5.462	4.979	5.524
89	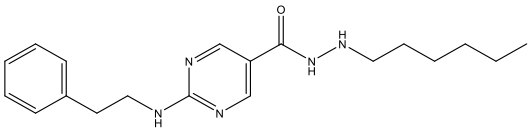	5.657	4.920	5.142	5.683	5.119	5.425
90	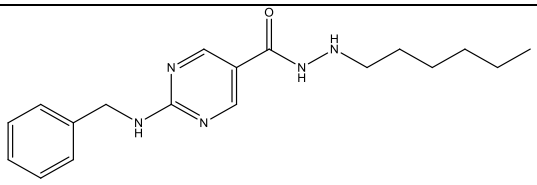	6.252	5.495	5.523	5.957	5.319	5.148
91	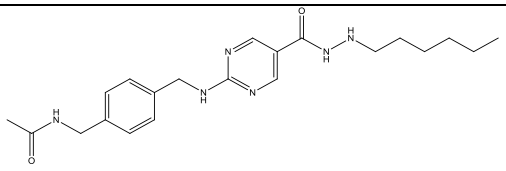	6.018	5.347	5.070	6.233	5.398	5.182

92	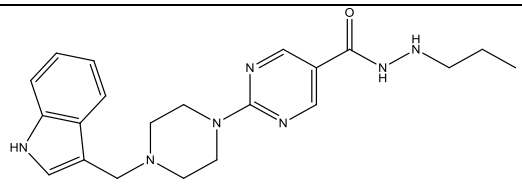	7.137	5.959	7.523	6.956	5.918	7.613
93	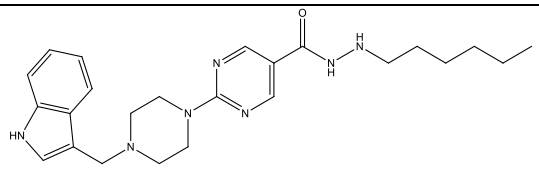	6.770	6.509	7	6.499	6.464	6.84
94	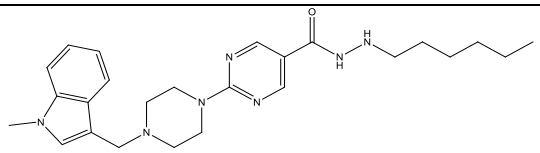	6.769	6.481	6.523	6.639	6.434	6.862
95	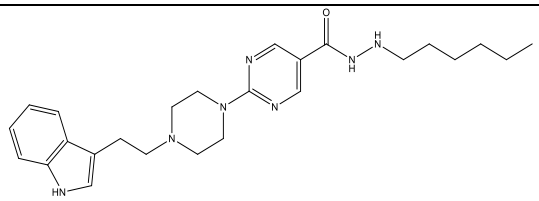	6.065	5.854	6	6.287	6.478	6.111
96	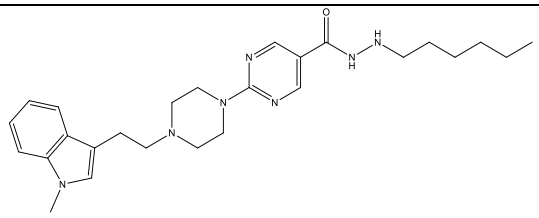	6.337	5.921	5.854	6.378	5.868	5.726
97	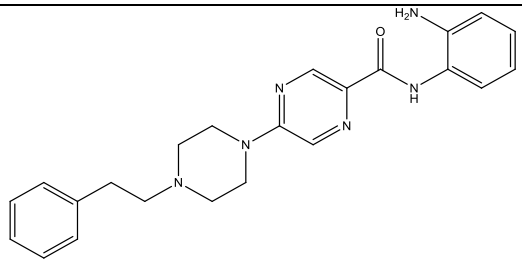	6.292	6.097	5.951	6.479	6.192	5.988

98	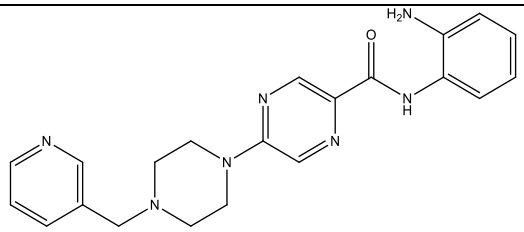	6.284	5.845	5.975	6.407	5.855	5.788
99	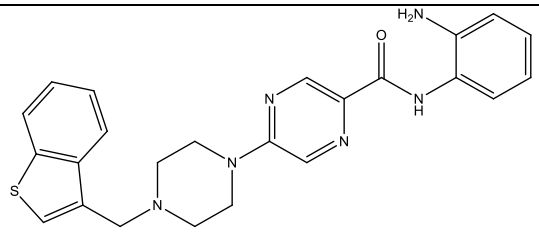	6.678	6.149	6.076	6.104	6.162	6.014
100	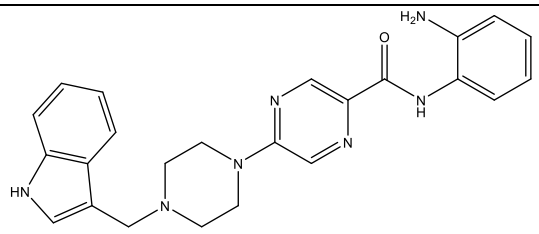	6.886	6.552	6.508	6.929	6.35	6.53
101	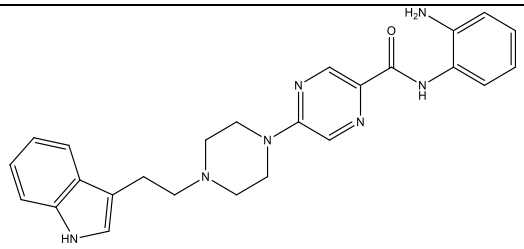	6.509	6.018	6.310	6.685	6.101	6.437
102	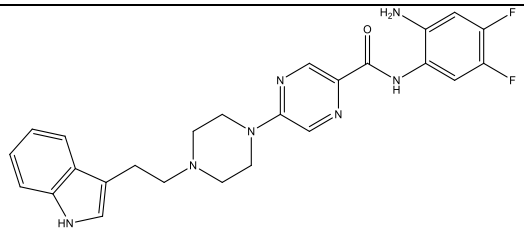	6.091	6.131	6.244	6.181	6.112	5.98
103	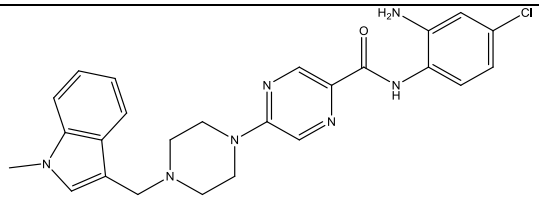	5.523	5.569	5.721	5.352	5.513	5.715

104	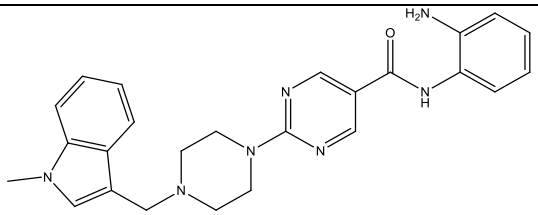	6.347	6.031	5.757	6.388	6.061	5.95
105	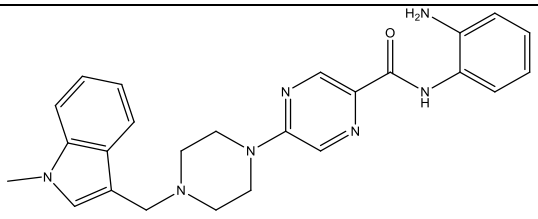	6.854	6.252	6.229	6.855	6.225	6.007
106	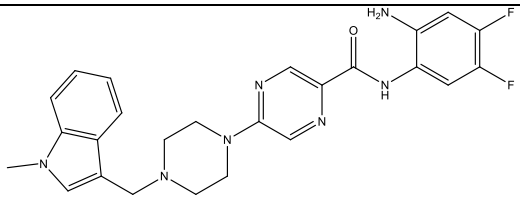	6.538	6.252	6.091	6.458	6.193	6.165
107	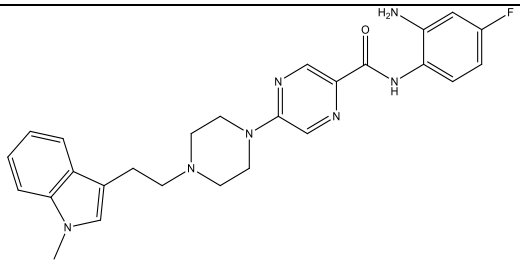	6.398	5.830	6.398	6.499	5.675	6.382
108	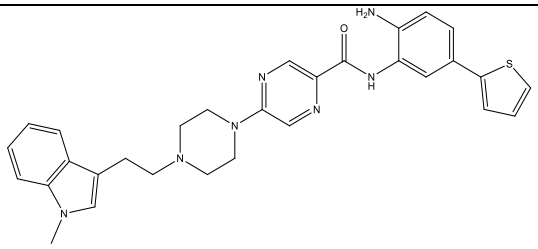	6.585	5.607	4.301	6.355	5.572	4.666
109	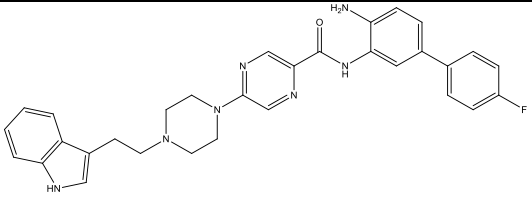	6.155	6.113	4.301	6.274	6.055	4.235

110	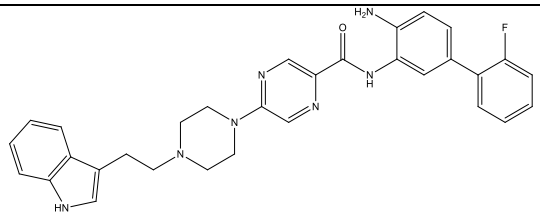	6.119	6.119	4.824	6.225	6.209	5.772
111	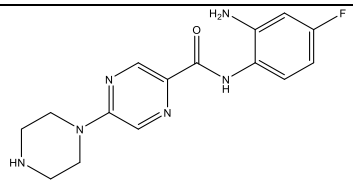	5.481	5.657	6.397	5.464	5.551	6.422
112	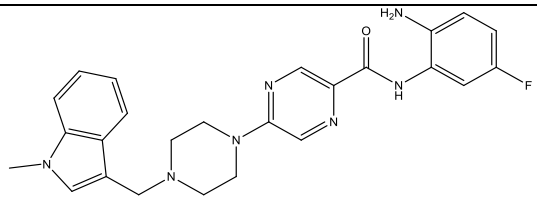	6.569	6.301	6.301	6.373	6.169	6.318
113	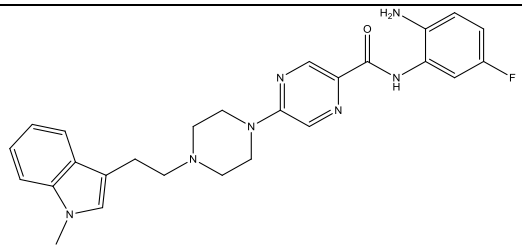	6.481	5.863	6.229	6.458	5.936	6.046
114	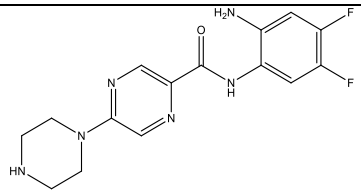	5.366	5.377	5.796	5.268	5.477	6.04
115	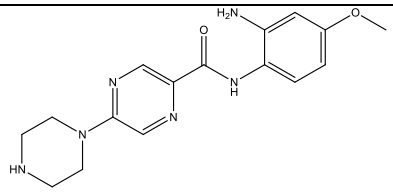	4.699	4.854	4.855	5.012	4.811	5.475
116	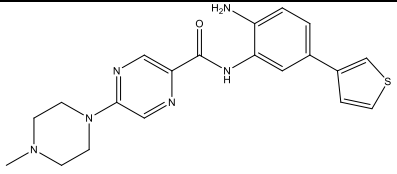	6.959	s6.745	5.356	7.047	6.325	5.211

117	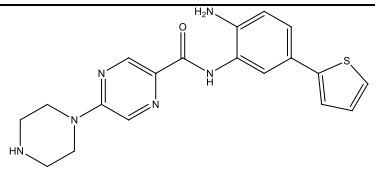	7.155	6.585	5.215	6.925	6.539	4.95
118	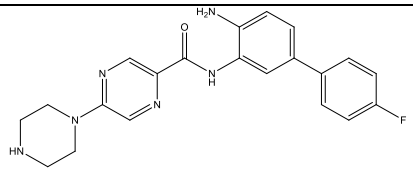	6.796	6.468	5.174	6.796	6.459	5.576
119	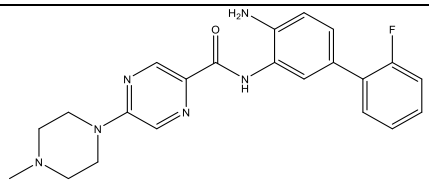	6.744	6.585	4.920	6.906	6.596	4.719
120	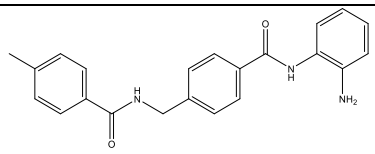	6.314	6.107	5.769	6.58	6.153	5.921
122	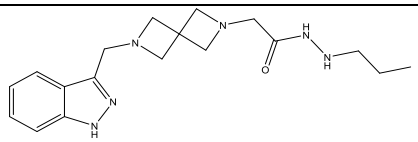	-	-	-	6.372	6.612	6.840
123	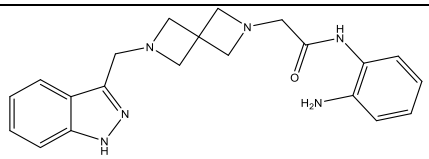	-	-	-	6.103	6.536	6.176
124	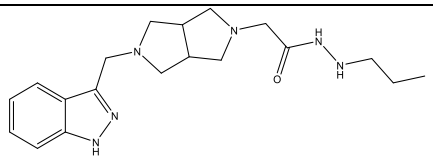	-	-	-	6.793	5.864	5.958
125	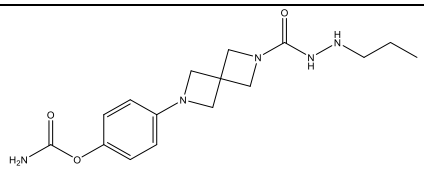	-	-	-	6.584	5.888	6.094

126	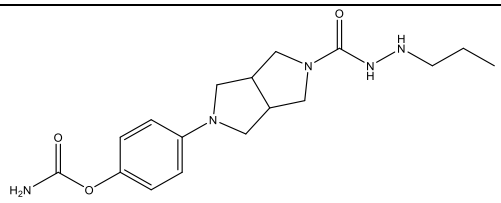	-	-	-	7.016	5.751	6.348

3.2. GRIND analysis

Three separate 3D-QSAR models were developed for each of the enzymes including HDAC1, 2, and 3. The constructed 3D-QSAR models were applied to analyze the GRIND variables as molecular determinants representor of the HDAC1-3 inhibitors. Figures 3 and Table 4 shows the distance dependent plot of PLS coefficients for the selected variables analyzed with 5LVs during 3D-QSAR model development. Based on the comparative study, five pair of GRIND descriptors with highest impact on pIC_{50} value of HDAC1, 2, and 3 enzymes were identified and analyzed. The identified variables includes DRY-DRY (6.8-7.2Å), O-TIP (1.6-2 Å), DRY-TIP (8–8.4 Å), DRY-N1 (2.8–3.2 Å), N1-TIP (6.4–6.8 Å) for HDAC1, DRY-TIP (16.8-17.2 Å), O-N1 (18-18.4 Å), N1-N1 (16-16.4 Å), O-N1 (14.8-15.2 Å), N1-TIP (18-18.4 Å) for HDAC2, and DRY-TIP (18.8-19.2 Å), DRY-N1 (1.6-2 Å), N1-TIP (4.8-5.2 Å), O-O (8-8.4 Å), O-TIP (6.8-7.2 Å) for HDAC3 with exact equal probe-probe distance. As it can be seen, there are some common variables between all or two isoenzymes including DRY-TIP and N1-TIP between HDAC1,2 and HDAC3, DRY-N1, O-TIP between HDAC1 and HDAC3. In the DRY-TIP variable, which negatively influences HDAC1 inhibitory activity, the DRY hydrophobic probe interacts with the cap section of the inhibitor. This probe is connected to TIP-interacting moieties at the core part of the compounds, with a separation of about 8–8.4 Å. This variable reflects how molecular conformation and folding affect biological activity, likely due to the positioning of the molecule within the active site of enzyme. The value of this descriptor is high in weak inhibitors (e.g., compounds **103**) and low in potent ones (**117** and **100**, Figure 4-A).

For HDAC2 and HDAC3, this variable describes interactions between a DRY probe in the cap region and a TIP probe at the opposite end of the inhibitor, exerting positive and negative impacts on inhibitory activity, respectively. This was confirmed as the value of the variable was high for compound **94** (Figure 4-B) and low for **114** in HDAC2, while high for **108** (k -C) and **109** in HDAC3. Thus, this GRIND variable may represent the optimal distance between the two ends of inhibitors, where the distance more or less than 6-8 atoms leads to reduced inhibitory activity. Another common variable, TIP-N1, describes an interaction between an HBD group located in the ZBG region and a TIP probe with the end of the molecule in the same area for HDAC1 (positive impact) and HDAC3 (negative impact). For HDAC2, this interaction occurs within the linker region and has a positive influence. High TIP-N1 values were found in compounds **86**, **87**, **119** (HDAC1) (Figure 4-D), **93** (HDAC2) (Figure 4-E), and **83**, **86** (HDAC3) (Figure 4-F). The differences in distance and the effect of DRY-TIP and TIP-N1 descriptors could thus help in designing selective inhibitors. The DRY-DRY GRIND variable is unique to HDAC1 (var17, 6.8–7.2 Å), showing a negative effect on HDAC1 inhibition. It represents the distance between two hydrophobic probes in the linker and cap regions. This variable appeared in all compounds and was particularly high in weak inhibitors (**103** (Figure 4-G), **101**, **112**, **102**) but nearly zero in potent ones (**117**, **116**, **118**). Such hydrophobic interactions may prevent the proper orientation of the inhibitor in the active site of the enzyme. The O-TIP descriptor highlights the importance of the presence of an HBD group located in 1.6–2 Å from a TIP-interacting moiety at the ZBG end, positively affecting HDAC1 inhibition. The presence of such HBD group in the ZBG section is essential to the formation of a pseudoring with zinc ion, for which the value of this variable was high for potent compounds like **117** (Figure 4-H) and **104** (Figure4). DRY-N1 pairs of variables explain the interaction of an HBA and a TIP

interacting probe in the linker region of the molecule, leading to decreased inhibitory activity (high in **89** (Figure 4-I), **90**, and low in **80**, **79**). The N1-N1 variable (var162) is unique to HDAC2 (16–16.4 Å) and negatively affects inhibition. It represents the interaction between two HBA interacting probes between the ZBG and cap regions, suggesting that this long distance may hinder proper orientation or cause unfavorable polar interactions at the enzyme rim. This descriptor was high in **98** (Figure 4-J), **91**, **79**, **80**, **115** compounds, which are almost weak to medium inhibitors, and was zero for the rest of the compounds. Two additional HDAC2-specific variables, O-N1 (var472, var464), with distances of 18–18.4 Å and 14.8–15.2 Å, show negative and positive effects on activity, respectively. Var472 (high in **98** (Figure 4-K), **115**) describes an HBD in the ZBG interacting with a nitrogen in the cap, while var464 (high in **97** (Figure 4-L), **98**, **104**) represents an HBD in the ZBG interacting with a nitrogen in the linker. A distance of 18–18.4 Å seems to hinder proper positioning, whereas 14.8–15.2 Å promotes favorable interactions with the active site of the enzyme. For HDAC3, the O-O variable (var81, 8–8.4 Å) negatively affects inhibition, being high in weak inhibitors (**119** (Figure 4-M), **97**) and representing an interaction between two HBDs in the ZBG region. Conversely, the O-TIP variable (6.8–7.2 Å) describes an HBD in the ZBG interacting with the end of the molecule, enhancing inhibition, which is high in potent compounds like **85** (Figure 4-N). Finally, the DRY-N1 descriptor highlights a hydrophobic–HBA interaction within the core or linker region (1.6–2 Å), which negatively impacts inhibitory activity which is high in less potent compounds like **88** (Figure 4-O). The results of classification-based 3D-QSAR study showed that just scaffolds containing benzamide or hydrazide serve as selective HDAC1-3 inhibitors, whereas hydroxamic acid derivatives do not show selectivity. The findings of GRIND based 3D-QSAR study alluded to the fact that the two crucial structural parameters for

HDAC inhibitory activity are presence of HBD groups in ZBD and the optimum distance between cap and ZBG. Consequently, the majority of the potent compounds were common among all three isoenzymes (HDAC1-3) such as **101**, **87**, and **93** which have pIC_{50} ≈6.5. However, only one compound (**108**) among our studied compounds was high selective inhibitor against HDAC1 isoenzyme with pIC_{50} value of 6 while has weak inhibitory activity against HDAC2 and HDAC3 with pIC_{50} value of 5.6 and 4.3, respectively. Based on the results of our study, there is a marginally selectivity between inhibition of isoenzymes which this issue was confirmed by near experimental IC_{50} values of inhibitors against HDAC1, 2, and, 3 also by high similarity between active site forms of these enzymes. Also, based on the obtained results of the developed 3D-QSAR models alongside the employment of the bioisosterism, 24 new molecules were designed. The designed molecules were docked on the active site of the HDAC2 enzyme to obtain an active conformation of the ligands. The inhibitory activity of designed compounds (pIC_{50}) was predicted using the developed models. Among them, five molecules showed high potency, whose structures (**122**-**126**) are shown in Table 2 also the poseview presentation of the interaction of the potent ligands with HDAC2 are presented as Figure S1 in supplementary material file. According to the structure of compounds, using indazole and carbamate group in the cap section, octahydropyrrolo[3,4-c]pyrrole and 2,6-diazaspiro[3.3]heptane in the linker lead to an increase in HDAC1-3 inhibition potency, while hydrazide or benzamide are as ZBG. Furthermore, compounds 122-126 could establish essential interactions with HDAC2 isoenzyme similar to those observed for entinostat experimentally. However, to achieve definitive results, there is a need to synthesis and evaluate the biological evaluation of the designed compounds.

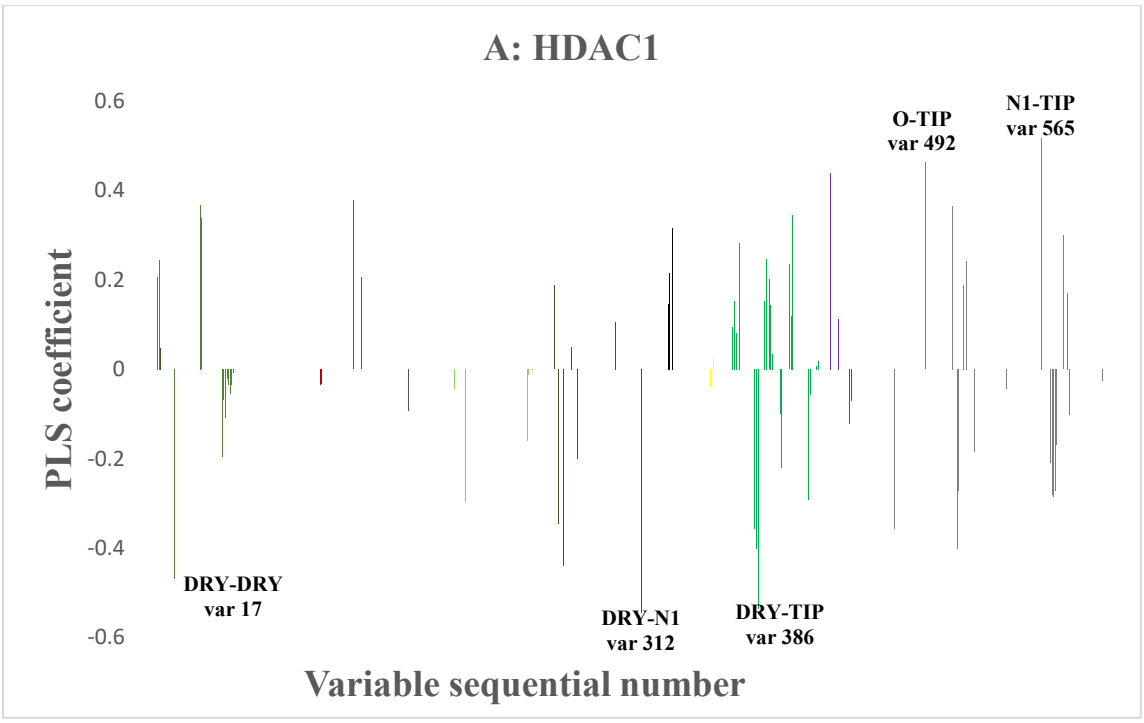
A: HDAC1
PLS coefficient
0.6
0.4
0.2
0
-0.2
-0.4
-0.6
DRY-DRY
var 17
DRY-N1
var 312
DRY-TIP
var 386
O-TIP
var 492
N1-TIP
var 565
Variable sequential number

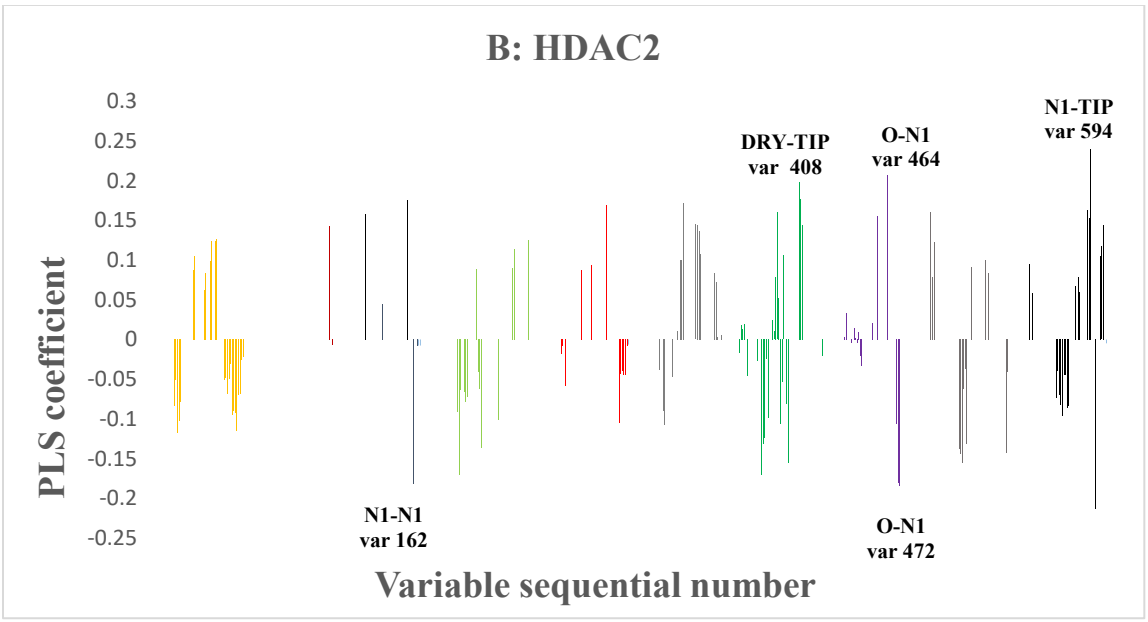
B: HDAC2
PLS coefficient
0.3
0.25
0.2
0.15
0.1
0.05
0
-0.05
-0.1
-0.15
-0.2
-0.25
N1-N1
var 162
DRY-TIP
var 408
O-N1
var 464
O-N1
var 472
N1-TIP
var 594
Variable sequential number

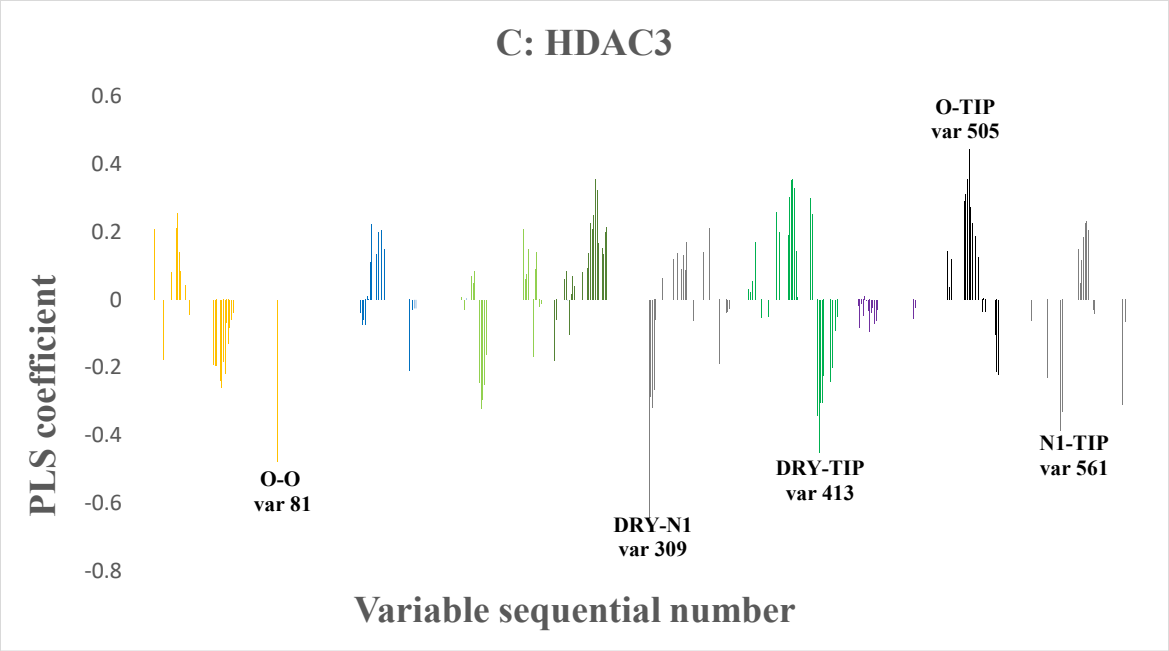

Figure 3. 5LV PLS coefficient plots for the obtained models. The most intensive variables are labeled by sequential numbers. 5LV indicates 5 latent variables; PLS, partial least squares; **A**: HDAC1, **B**. HDAC2. **C**. HDAC3.

As well as, a brief structure – activity relationship was performed on 43 selected selective HDAC1-3 inhibitors. From all collected structures (121 compounds) those which have benzamide or hydrazide as ZBG were filtered as selective HDAC1-3 inhibitors with diverse cap and linker groups. In compounds with core structure of pyrazine (linker) to 2-aminobenzamide (linker)[39], presence of 3-indolyl in the cap group (compounds **92**, **93**, and **94**) leads to increases inhibitory activity against HDAC1, -2, and -3. Also, the results showed that substitution of methyl linking cap group and pyrazine to ethyl (compound **101**) decreases inhibition potency. Furthermore, replacement of pyrazine linker (compound **105**) with pyrimidine (compound **104**) significantly reduces the inhibitory activity. As well as it is worth to note that compounds which has 2-thienyl group in the position-5 of 2-aminobenzamide leads to selectivity of inhibitor to HDAC1, -2 (compounds **108**, **117**). About compounds containing alkyl hydrazide in ZBG[23], findings showed that the optimum size of alkyl group in alkyl hydrazide moiety (in ZBG) was three carbons to occupy the foot-pocket

in which enhances inhibition activity and selectivity against HDAC3 specifically those have 3-indolyl (compound **92**) or benzyl (compound **85**) in their cap group. Also in compounds which acetamidomethyl was attached to their terminal group in cap group leads to decrease inhibition activity to HDAC3.

Table 4. The most important structural variables in the 3D-QSAR models for HDAC1, 2, and 3-selective inhibitors.

Isoenzyme	variable	Distance(A)	Probe block	value	Interaction between structural elements	Comment
HDAC1	492	1.6 - 2	O-TIP	0.463	NH in ZBG and ZBG ends of inhibitor	For 37 compounds, higher positive impact on active compounds
	17	6.8 - 7.2	DRY-DRY	-0.469	Aromatic groups in cap and linker	For all compounds, higher negative impact on less active compounds
	386	8 – 8.4	DRY-TIP	-0.536	Hydrophobic groups in cap and linker	For all compounds, higher negative impact on less active compounds
	312	2.8 – 3.2	DRY-N1	-0.545	Nitrogen and aromatic group in linker	For all compounds, higher negative impact on less active compounds
	565	6.4 – 6.8	N1-TIP	0.519	HBD in ZBG and end of inhibitor	For all compounds, higher positive impact on active compounds
HDAC2	472	18 - 18.4	O-N1	-0.185	HBA in cap and HBD in ZBG	For 2 compounds (96,115), higher negative impact on less active compounds
	464	14.8 - 15.2	O-N1	0.207	HBD in ZBG and HBA in piperazine(linker)	For 35 compounds, higher positive impact on active compounds
	408	16.8 - 17.2	DRY-TIP	0.198	Two ends of inhibitor	For all compounds, higher positive impact on active compounds
	162	16 - 16.4	N1-N1	-0.182	Two HBD in ZBG and cap	For 5 compounds, higher negative impact on less active compounds
	594	18 - 18.4	N1-TIP	0.239	Nitrogen of piperazine (linker) and end of inhibitor(ZBG)	For 37 compounds, higher positive impact on active compounds
HDAC3	413	18.8-19.2	DRY-TIP	-0.451	Two ends of molecule	For all except 5 compounds(85,111,114,116,84), higher negative impact on less active compounds
	505	6.8-7.2	O-TIP	0.443	HBD in ZBG and end of ZBG	For all compounds, higher positive impact on active compounds
	309	1.6-2	DRY-N1	-0.643	Nitrogen and aromatic group in linker	For 36 compounds, higher negative impact on less active compounds
	81	8-8.4	O-O	-0.477	Two HBD in ZBG	For 38 compounds, higher negative impact on less active compounds
	561	4.8-5.2	N1-TIP	-0.386	Nitrogen in cap and end of cap	For all except 1 compound(102), higher negative impact on less active compounds

A

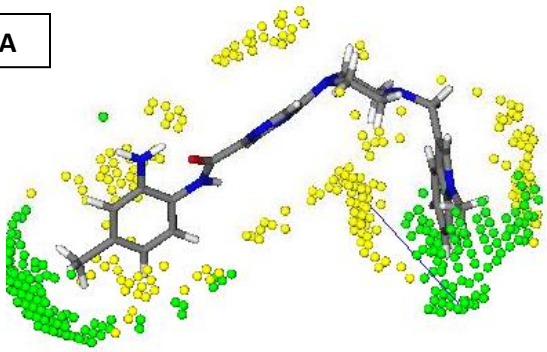

B

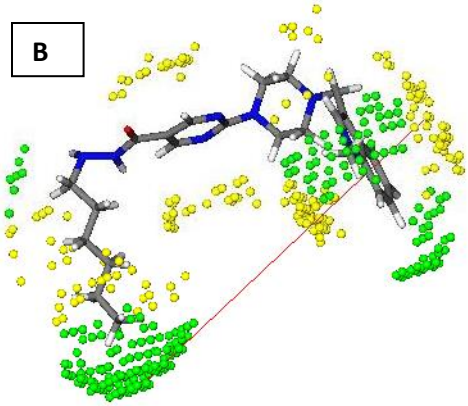

C

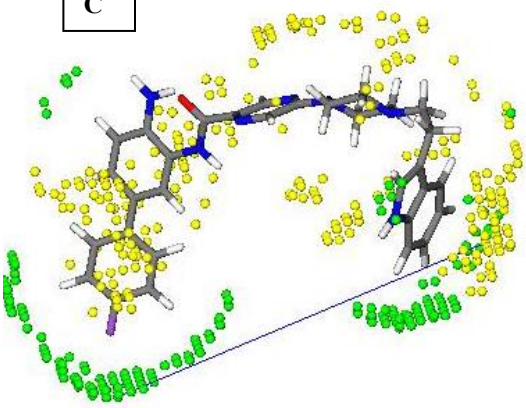

D

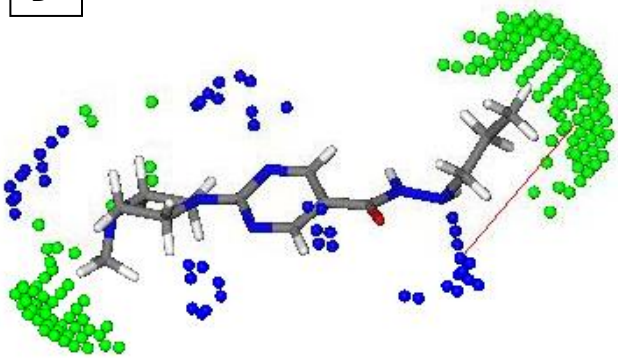

E

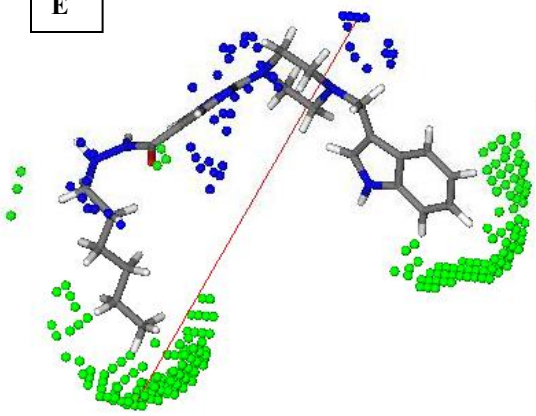

F

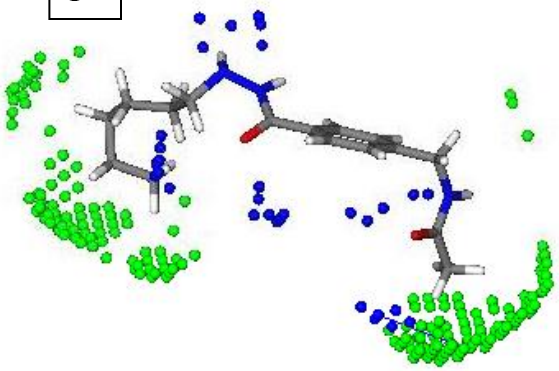

G

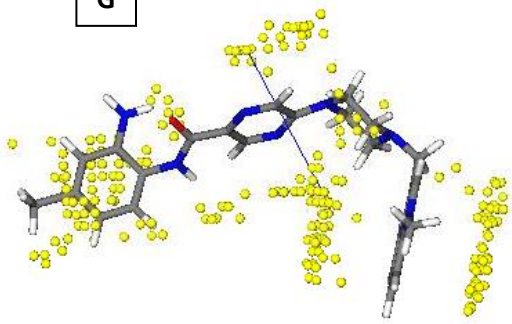

H

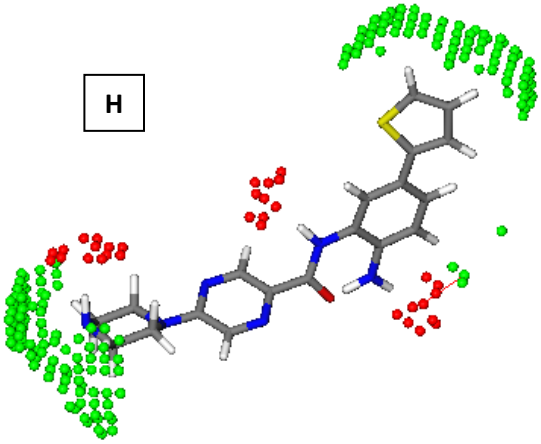

I

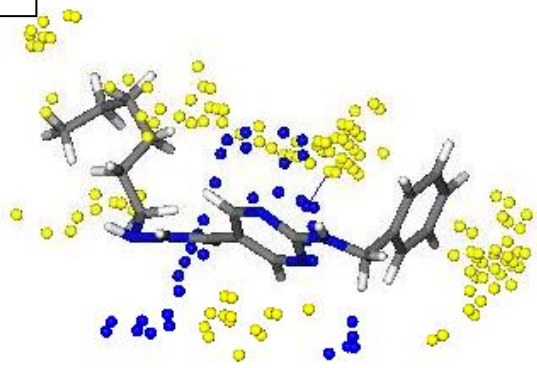

J

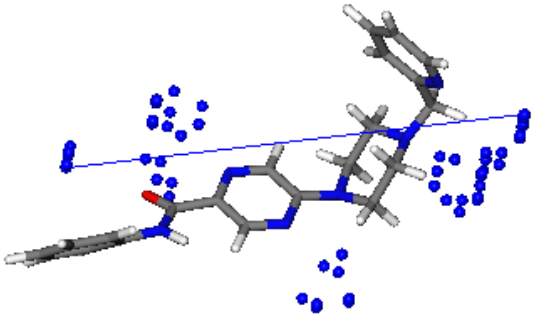

K

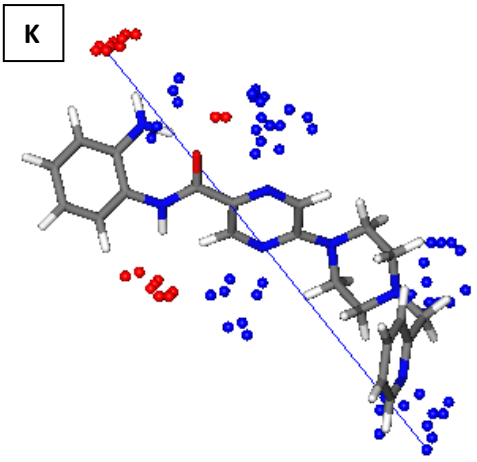

L

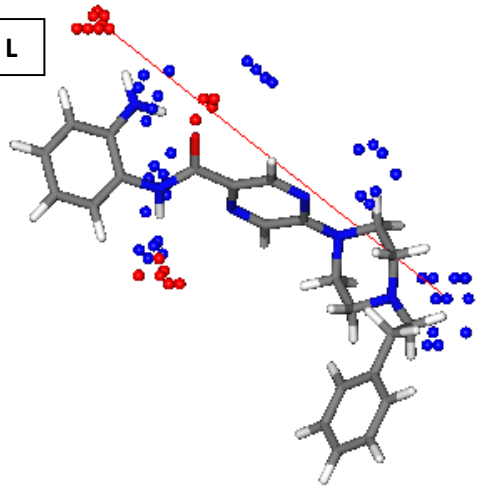

M

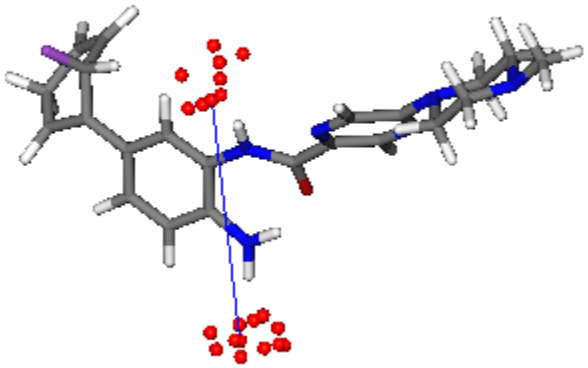

N

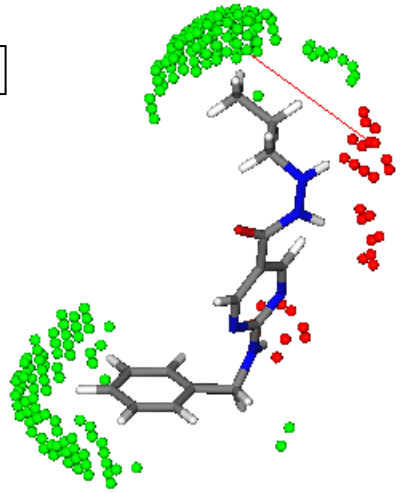

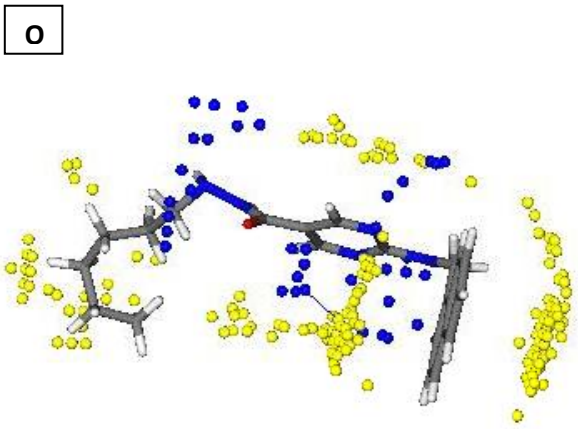

Figure 4. The most important structural elements associated with variables: **A**. DRY-TIP (compound **103**) for HDAC1; **B**. DRY-TIP (compound **94**) for HDAC2; **C**. DRY-TIP (compound **109**) for HDAC3; **D**. N1-TIP (compound **86**) for HDAC1; **E**. N1-TIP (compound **93**) for HDAC2; **F**. N1-TIP (compound **83**) for HDAC3; **G**. DRY-DRY (compound **103**) for HDAC1; **H**. O-TIP (compound **117**) for HDAC1; **I**. DRY-N1 (compound **90**) for HDAC1; **J**. N1-N1 (compound **98**) for HDAC2; **K**. O-N1 (var472_compound **98**) for HDAC2; **L**. O-N1 (var464_compound **97**) for HDAC2; **M**. O-O (compound **119**) for HDAC3; **N**. O-TIP (compound **109**) for HDAC3; **O**. DRY-N1 (compound **109**) for HDAC3;

3.3. Predictivity power of the GRIND-based model

For building 3D-QSAR models, initially, the compounds were divided into train and test sets using SPSS program. To this, the random sample selection prompt was used to select test set (about 20%) in an effort to have similar range of biological activities (pIC_{50}) for both sets. The train compounds were subjected to Pentacle program and the generated GRIND-based descriptors were used to build QSAR models. Fractional factorial design (FFD) variable selection was performed for several times on the generated models until no significant changes in statistical indices (r^2, q^2, and SDEP) were observed. The internal predictivity of the models was evaluated by LOO (leave-one-out) method and the obtained statistics are shown in Table 3. The best model was selected based on R^2_{acc} and Q^2_{acc} values with 5 LV and good predictive power of constructed model (Q^2 external > 0.5)[54]. The external Q^2 was obtained from plotting experimental HDAC1,2,3 inhibition activity values (pIC_{50}) versus predicted values for test set in an excel program. As well as, three scatter diagrams were created to evaluation of correlation of experimental values versus predicted values of compounds. Based on the scatter plots which are shown in Figure 5, the close distribution of the two data sets showed that the 3D-QSAR models had reliability and acceptable prediction ability.

Table 3. Statistical results of developed 3D-QSAR model.

Criteria	Isoenzyme	R^2_{acc}	Q^2_{acc}	SDEP	$R^2_{obs.\ vs\ pred.}$
Internal validation parameters	HDAC1	0.90	0.62	0.30	0.79
	HDAC2	0.98	0.84	0.21	0.76
	HDAC3	0.97	0.83	0.36	0.78
Criteria	Isoenzyme	Q^2			
External validation parameters	HDAC1	0.72			
	HDAC2	0.90			
	HDAC3	0.82			

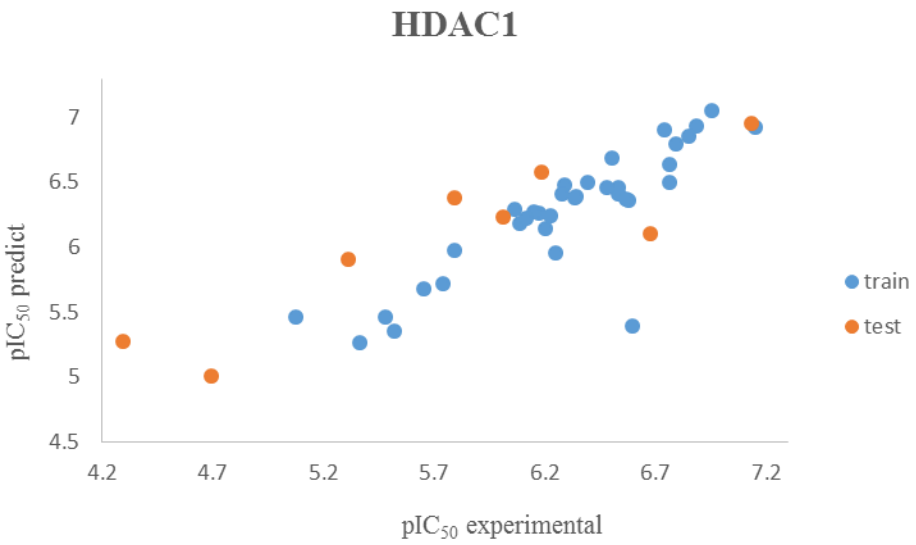
HDAC1
7
6.5
6
5.5
5
4.5
4.2
4.7
5.2
5.7
6.2
6.7
7.2
pIC50 predict
pIC50 experimental
train
test

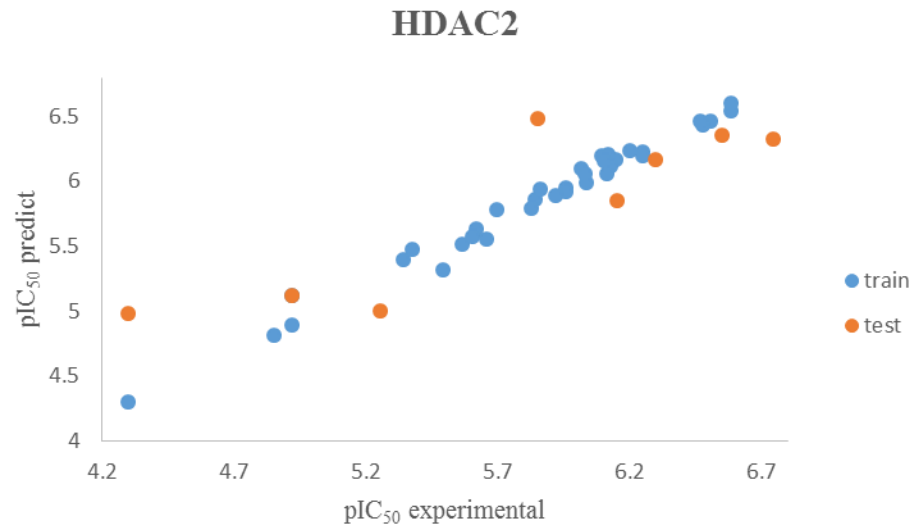
HDAC2
6.5
6
5.5
5
4.5
4
4.2
4.7
5.2
5.7
6.2
6.7
pIC50 predict
pIC50 experimental
train
test

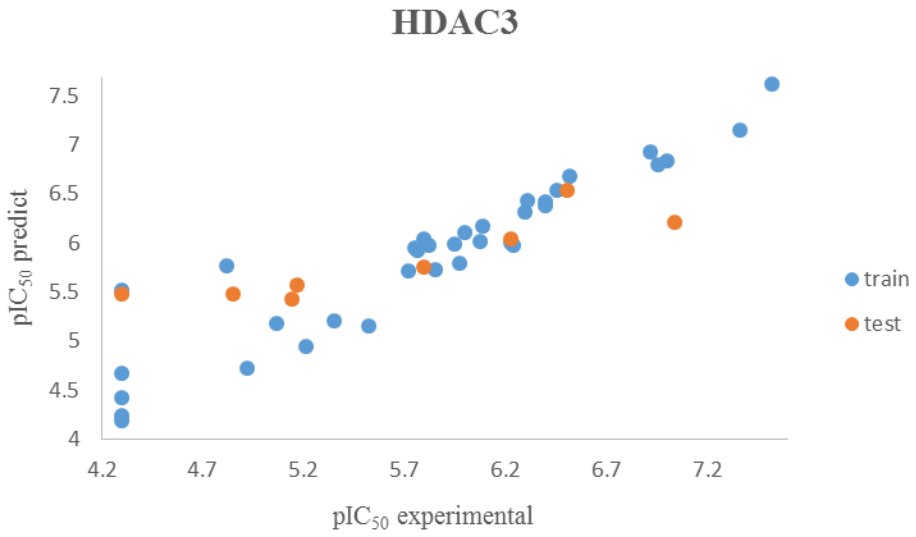

Figure 5. Experimental vs predicted pIC_{50} for compounds. Blue squares indicate training set and orange squares show the test set compounds

4. Conclusions

In summary, in this study a classification based QSAR was executed on a series of HDAC inhibitors to identify selective HDAC1-3 inhibitors. In the next step, three separate alignment-independent 3D-QSAR studies were executed on 43 selected compounds containing benzamide or hydrazide scaffolds for the inhibitory activity of HDAC isoforms 1-3. According to obtained results, the constructed models could predict the inhibitory activity of compounds with reliable statistics. The key structural areas effect on the biological activity of the selective inhibitors are (i) the presence of two HBD groups in ZBD to chelate to zinc ion of the enzyme, and (ii) the optimum distance of 8 atom carbons between ZBG and cap groups. The results of classification confirmed the obtained finding, i.e., compounds with benzamide or hydrazide groups as ZBD were identified as selective HDAC1-3 inhibitors, and all selected compounds have optimum distance between ZBG and cap groups. Moreover, there are marginal selectivity between HDAC1, 2, and 3 which

showed there similarity. The result of this work can be used for designing novel series of selective HDAC1-3 inhibitors with desired activity.

5. **Author Contributions:** The article was co-written by all authors. The final draft has been approved by all authors. Nasri. A. and Cheshmazar. N. (Investigation and Writing - Original Draft), Dastmalchi. S. (Supervision and Review & Editing).

6. **Acknowledgments:** The authors thank the Research Office and Biotechnology Research Center of Tabriz University of Medical Sciences for providing financial support under the Postgraduate Research Grant scheme for the master of Amirhossein Nasri (Grant number 75134).

7. **Competing interests:** The authors declare no competing financial interest.

8. References

1. Ali I, Conrad RJ, Verdin E, Ott MJCr. Lysine acetylation goes global: From epigenetics to metabolism and therapeutics. *Chem Rev*. 2018;118(3):1216-52. doi: 10.1021/acs.chemrev.7b00181.
2. Narita T, Weinert BT, Choudhary CJNrMcb. Functions and mechanisms of non-histone protein acetylation. *Nat Rev Mol Cell Biol*. 2019;20(3):156-74. doi: 10.1038/s41580-018-0081-3.
3. Greco TM, Yu F, Guise AJ, Cristea IMJM, Proteomics C. Nuclear import of histone deacetylase 5 by requisite nuclear localization signal phosphorylation. *Mol Cell Proteomics*. 2011;10(2):S1-S15. doi: 10.1074/mcp.M110.004317.
4. Sahakian E, Chen J, Powers JJ, Chen X, Maharaj K, Deng SL, et al. Essential role for histone deacetylase 11 (hdac11) in neutrophil biology. *J Leukoc Biol*. 2017;102(2):475-86. doi: 10.1189/jlb.1A0415-176RRR.
5. Hildmann C, Riester D, Schwienhorst AJAm, biotechnology. Histone deacetylases—an important class of cellular regulators with a variety of functions. *Appl Microbiol Biotechnol.* 2007;75:487-97. doi: 10.1007/s00253-007-0911-2.
6. Zagni C, Floresta G, Monciino G, Rescifina AJMrr. The search for potent, small-molecule hdacis in cancer treatment: A decade after vorinostat. *Med Res Rev*. 2017;37(6):1373-428. doi: 10.1002/med.21437.
7. Ganai SA. Histone deacetylase inhibitors-epidrugs for neurological disorders: Springer; 2019.
8. Lee J-H, Bollschweiler D, Schäfer T, Huber RJSa. Structural basis for the regulation of nucleosome recognition and hdac activity by histone deacetylase assemblies. *Sci Adv.* 2021;7(2):eabd4413. doi: 10.1126/sciadv.abd4413.

9. Cheshmazar N, Hamzeh-Mivehroud M, Charoudeh HN, Hemmati S, Melesina J, Dastmalchi SJLS. Current trends in development of hdac-based chemotherapeutics. *Life Sci.* 2022;308:120946. doi: 10.1016/j.lfs.2022.120946.
10. Falkenberg KJ, Johnstone RWJNrDd. Histone deacetylases and their inhibitors in cancer, neurological diseases and immune disorders. *Nat Rev Drug Discov.* 2014;13(9):673-91. doi: 10.1038/nrd4360.
11. Zwergel C, Stazi G, Valente S, Mai AJJCE. Histone deacetylase inhibitors: Updated studies in various epigenetic-related diseases. *J Clin Epigenetics.* 2016;2(1):7.
12. Bolden JE, Peart MJ, Johnstone RWJNrDd. Anticancer activities of histone deacetylase inhibitors. *Nat Rev Drug Discov.* 2006;5(9):769-84. doi: 10.1038/nrd2133.
13. Dovey OM, Foster CT, Conte N, Edwards SA, Edwards JM, Singh R, et al. Histone deacetylase 1 and 2 are essential for normal t-cell development and genomic stability in mice. *Blood.* 2013;121(8):1335-44. doi: 10.1182/blood-2012-07-441949.
14. Heideman MR, Wilting RH, Yanover E, Velds A, de Jong J, Kerkhoven RM, et al. Dosage-dependent tumor suppression by histone deacetylases 1 and 2 through regulation of c-myc collaborating genes and p53 function. *Blood.* 2013;121(11):2038-50. doi: 10.1182/blood-2012-08-450916.
15. Santoro F, Botrugno OA, Dal Zuffo R, Pallavicini I, Matthews GM, Cluse L, et al. A dual role for hdac1: Oncosuppressor in tumorigenesis, oncogene in tumor maintenance. *Blood.* 2013;121(17):3459-68. doi: 10.1182/blood-2012-10-461988.
16. Yang S-s, Zhang R, Wang G, Zhang Y-fJTn. The development prospection of hdac inhibitors as a potential therapeutic direction in alzheimer's disease. *Transl Neurodegener.* 2017;6:1-6. doi: 10.1186/s40035-017-0089-1.
17. Ediriweera MK, Cho SKJP, therapeutics. Targeting mirnas by histone deacetylase inhibitors (hdaci): Rationalizing epigenetics-based therapies for breast cancer. *Pharmacol Ther*. 2020;206:107437. doi: 10.1016/j.pharmthera.2019.107437.
18. Souza LÂ, Bastos MS, Agripino JdM, Onofre TS, Cala LFA, Heimburg T, et al. Histone deacetylases inhibitors as new potential drugs against leishmania braziliensis, the main causative agent of new world tegumentary leishmaniasis. *Biochem Pharmacol.* 2020. doi: 10.1016/j.bcp.2020.114191.
19. Li Y, Seto EJCSHpim. Hdacs and hdac inhibitors in cancer development and therapy. *Cold Spring Harb Perspect Med* 2016;6(10):a026831. doi: 10.1101/cshperspect.a026831.
20. Pan H, Cao J, Xu WJA-CAiMC-A-CA. Selective histone deacetylase inhibitors. *Anti-Cancer Agents Med Chem.* 2012;12(3):247-70. doi: 10.2174/187152012800228814.
21. Luo Y, Li HJIjoms. Structure-based inhibitor discovery of class i histone deacetylases (hdacs). *Int J Mol Sci*. 2020;21(22):8828. doi: 10.3390/ijms21228828.
22. Cheshmazar N, Hamzeh-Mivehroud M, Hemmati S, Abolhasani H, Heidari F, Charoudeh HN, et al. Key structural requirements of benzamide derivatives for histone deacetylase inhibition: Design, synthesis and biological evaluation. *Future Med Chem*. 2024;16(9):859-72. doi: 10.4155/fmc-2023-0122.
23. Sun P, Wang J, Khan KS, Yang W, Ng BW-L, Ilment N, et al. Development of alkylated hydrazides as highly potent and selective class i histone deacetylase inhibitors with t cell modulatory properties. *J Med Chem*. 2022;65(24):16313-37. doi: 10.1021/acs.jmedchem.2c01132.
24. Muratov EN, Bajorath J, Sheridan RP, Tetko IV, Filimonov D, Poroikov V, et al. Qsar without borders. *Chem Soc Rev*. 2020;49(11):3525-64. doi: 10.1039/d0cs00098a.
25. Neves BJ, Braga RC, Melo-Filho CC, Moreira-Filho JT, Muratov EN, Andrade CHJFip. Qsar-based virtual screening: Advances and applications in drug discovery. *Front Pharmacol.* 2018;9:1275. doi: 10.3389/fphar.2018.01275.
26. Hamzeh-Mivehroud M, Sokouti B, Dastmalchi S. An introduction to the basic concepts in qsar-aided drug design. *Artif Intell* ; 2017. p. 32-78.
27. Roy K, Kar S, Ambure P. On a simple approach for determining applicability domain of qsar models. *Chemom Intell Lab Syst*. 2015;145:22-9. doi: 10.1016/j.chemolab.2015.04.013.

28. Verma J, Khedkar VM, Coutinho ECJCtimc. 3d-qsar in drug design-a review. *Curr Top Med Chem.* 2010;10(1):95-115. doi: 10.2174/156802610790232260.
29. Halder AK, Moura AS, Cordeiro MNDJEootp. Qsar modelling: A therapeutic patent review 2010-present. *Expert Opin Ther Pat*. 2018;28(6):467-76. doi: 10.1080/13543776.2018.1475560.
30. Wilkes JG, Stoyanova-Slavova IB, Buzatu DAJJoc-amd. Alignment-independent technique for 3d qsar analysis. *J Comput Aided Mol Des*. 2016;30:331-45. doi: 10.1007/s10822-016-9909-0.
31. Pastor M, Cruciani G, McLay I, Pickett S, Clementi S. Grid-independent descriptors (grind): A novel class of alignment-independent three-dimensional molecular descriptors. *J Med Chem*. 2000;43(17):3233-43. doi: 10.1021/jm000941m.
32. Goodford PJ. A computational procedure for determining energetically favorable binding sites on biologically important macromolecules. *J Med Chem*. 1985;28(7):849-57. doi: 10.1021/jm00145a002.
33. Artese A, Cross S, Costa G, Distinto S, Parrotta L, Alcaro S, et al. Molecular interaction fields in drug discovery: Recent advances and future perspectives. *Wiley Interdiscip Rev Comput Mol Sci*. 2013;3(6):594-613. doi: 10.1002/wcms.1150.
34. Bayer T, Chakrabarti A, Lancelot J, Shaik TB, Hausmann K, Melesina J, et al. Synthesis, crystallization studies, and in vitro characterization of cinnamic acid derivatives as smhdac8 inhibitors for the treatment of schistosomiasis. *ChemMedChem.* 2018;13(15):1517-29. doi: 10.1002/cmdc.201800238.
35. Cheshmazar N, Hemmati S, Hamzeh-Mivehroud M, Sokouti B, Zessin M, Schutkowski M, et al. Development of new inhibitors of hdac1–3 enzymes aided by in silico design strategies. *J Chem Inf Mode*l. 2022;62(10):2387-97. doi: 10.1021/acs.jcim.1c01557.
36. Darwish S, Ghazy E, Heimburg T, Herp D, Zeyen P, Salem-Altintas R, et al. Design, synthesis and biological characterization of histone deacetylase 8 (hdac8) proteolysis targeting chimeras (protacs) with anti-neuroblastoma activity. *Int J Mol Sci.* 2022;23(14):7535. doi: 10.3390/ijms23147535.
37. Ghazy E, Zeyen P, Herp D, Hügle M, Schmidtkunz K, Erdmann F, et al. Design, synthesis, and biological evaluation of dual targeting inhibitors of histone deacetylase 6/8 and bromodomain brpf1. *Eur J Med Chem*. 2020;200:112338. doi: 10.1016/j.ejmech.2020.112338.
38. Heimburg T, Kolbinger FR, Zeyen P, Ghazy E, Herp D, Schmidtkunz K, et al. Structure-based design and biological characterization of selective histone deacetylase 8 (hdac8) inhibitors with anti-neuroblastoma activity. *J Med Chem.* 2017;60(24):10188-204. doi: 10.1021/acs.jmedchem.7b01447.
39. Ibrahim HS, Abdelsalam M, Zeyn Y, Zessin M, Mustafa A-HM, Fischer MA, et al. Synthesis, molecular docking and biological characterization of pyrazine linked 2-aminobenzamides as new class i selective histone deacetylase (hdac) inhibitors with anti-leukemic activity. *Int J Mol Sci.* 2021;23(1):369. doi: 10.3390/ijms23010369.
40. Senger J, Melesina J, Marek M, Romier C, Oehme I, Witt O, et al. Synthesis and biological investigation of oxazole hydroxamates as highly selective histone deacetylase 6 (hdac6) inhibitors. *J Med Chem*. 2016;59(4):1545-55. doi: 10.1021/acs.jmedchem.5b01493.
41. Simoben CV, Robaa D, Chakrabarti A, Schmidtkunz K, Marek M, Lancelot J, et al. A novel class of schistosoma mansoni histone deacetylase 8 (hdac8) inhibitors identified by structure-based virtual screening and in vitro testing. *Molecules* 2018;23(3):566. doi: 10.3390/molecules23030566.
42. Vögerl K, Ong N, Senger J, Herp D, Schmidtkunz K, Marek M, et al. Synthesis and biological investigation of phenothiazine-based benzhydroxamic acids as selective histone deacetylase 6 inhibitors. *J Med Chem*. 2019;62(3):1138-66. doi: 10.1021/acs.jmedchem.8b01090.
43. Allinger NL. Conformational analysis. 130. Mm2. A hydrocarbon force field utilizing v1 and v2 torsional terms. *J Am Chem Soc*. 1977;99(25):8127-34. doi: 10.1021/ja00467a001.
44. Dewar MJ, Thiel W. Ground states of molecules. 39. Mndo results for molecules containing hydrogen, carbon, nitrogen, and oxygen. *J Am Chem Soc.* 1977;99(15):4907-17. doi: 10.1021/ja00457a005.
45. O'Boyle NM, Banck M, James CA, Morley C, Vandermeersch T, Hutchison GR. Open babel: An open chemical toolbox. *J Cheminform*. 2011;3:1-14. doi: 10.1186/1758-2946-3-33.

46. Roy K. Quantitative structure-activity relationships (qsars): A few validation methods and software tools developed at the dtc laboratory. *J Indian Chem Soc*. 2018;95(12):1497-502.
47. Ruijter AJd, GENNIP AHv, Caron HN, Kemp S, KUILENBURG ABvJBJ. Histone deacetylases (hdacs): Characterization of the classical hdac family. *Biochem J*. 2003;370(3):737-49. doi: 10.1042/bj20021321.
48. Johansson MU, Zoete V, Michielin O, Guex N. Defining and searching for structural motifs using deepview/swiss-pdbviewer. *BMC bioinformatics* 2012;13:1-11. doi: 10.1186/1471-2105-13-173.
49. Jones G, Willett P, Glen RC. Molecular recognition of receptor sites using a genetic algorithm with a description of desolvation. *J Mol Biol*. 1995;245(1):43-53. doi: 10.1016/s0022-2836(95)80037-9.
50. Morris GM, Goodsell DS, Halliday RS, Huey R, Hart WE, Belew RK, et al. Automated docking using a lamarckian genetic algorithm and an empirical binding free energy function. *J Comput Chem*. 1998;19(14):1639-62. doi: 10.1002/(SICI)1096-987X(19981115)19:14<1639::AID-JCC10>3.0.CO;2-B.
51. Lauffer BE, Mintzer R, Fong R, Mukund S, Tam C, Zilberleyb I, et al. Histone deacetylase (hdac) inhibitor kinetic rate constants correlate with cellular histone acetylation but not transcription and cell viability. *J Biol Chem*. 2013;288(37):26926-43. doi: 10.1074/jbc.M113.490706.
52. Duran A, Martínez GC, Pastor M. Development and validation of amanda, a new algorithm for selecting highly relevant regions in molecular interaction fields. *J Chem Inf Model*. 2008;48(9):1813-23. doi: 10.1021/ci800037t.
53. Roy K, Kar S, Das RN. Qsar/qspr modeling fundamental concepts. doi: 10.1007/978-3-319-17281-1
54. Golbraikh A, Tropsha AJJomg, modelling. Beware of q2. *J Mol Graph Model.* 2002;20(4):269-76. doi: 10.1016/s1093-3263(01)00123-1.